Microscopy, 2024, **73(5)**, 439–445
DOI: https://doi.org/10.1093/jmicro/dfae021
Advance Access Publication Date: 25 April 2024
Article

MICROSCOPY

Spin polarization of photoelectrons emitted from spin-orbit coupled surface states of Pb/Ge(111)

Koichiro Yaji[1,*], **Kenta Kuroda**[2,3], **Shunsuke Tsuda**[1] and **Fumio Komori**[1]

[1]Center for Basic Research on Materials, National Institute for Materials Science, 3-13 Sakura, Tsukuba, Ibaraki 305-0003, Japan
[2]Graduate School of Advanced Science and Engineering, Hiroshima University, 1-3-1 Kagamiyama, Higashi-Hiroshima 739-8526, Japan
[3]International Institute for Sustainability with Knotted Chiral Meta Matter (WPI-SKCM^2), Hiroshima University, 1-3-1 Kagamiyama, Higashi-Hiroshima 739-8526, Japan
[*]To whom correspondence should be addressed. E-mail: yaji.koichiro@nims.go.jp

Abstract

We report that the spin vector of photoelectrons emitted from an atomic layer Pb grown on a germanium substrate [Pb/Ge(111)] can be controlled using an electric field of light. The spin polarization of photoelectrons excited by a linearly polarized light is precisely investigated by spin- and angle-resolved photoemission spectroscopy. The spin polarization of the photoelectrons observed in the mirror plane reverses between p- and s-polarized lights. Considering the dipole transition selection rule, the surface state of Pb/Ge(111) is represented by a linear combination of symmetric and asymmetric orbital components coupled with spins in mutually opposite directions. The spin direction of the photoelectrons is different from that of the initial state when the electric field vector of linearly polarized light deviates from p- or s-polarization conditions. The quantum interference in the photoexcitation process can determine the direction of the spin vector of photoelectrons.

Key words: spin polarization, surface state, spin-orbit coupling, quantum interference, spin- and angle-resolved photoemission spectroscopy, Pb/Ge(111)

Introduction

Spintronics utilizing both charge and spin has been intensively studied because of the potential for high-speed and energy-saving devices. It is essential to control the spin direction to apply electron spin in devices, typically achieved through external magnetic fields, electric fields, lights and heat. On the other hand, electrons exhibit wave-like characteristics, allowing them to undergo superposition and interference. According to quantum mechanics, the superposition of spin-up and spin-down states can yield an arbitrarily oriented spin state. Spin control using coherent spin has been proposed and demonstrated in qubits so far [1,2], and their practical applications are anticipated in future quantum computing and quantum communication [3].

In a general consequence of the spin-orbit coupled systems, such as topological insulators and Rashba spin-split systems, the spin and momentum of the surface states are strongly coupled to each other, and the surface state exhibits helical spin texture, the so-called spin-momentum locking (Fig. 1a). In more detail, the direction of the spin vector depends on the symmetry of the orbital wavefunctions due to the spin-orbit coupling [4–9]. In particular, the symmetric and asymmetric parts of the wavefunction are coupled to spins pointing to mutually opposite directions when the system has mirror symmetry (Fig. 1b) [10]. This has been demonstrated experimentally and theoretically in Bi(111) and Bi_2Se_3(111), in which the spin polarizations of photoelectrons emitted from the surface states by p- and s-polarized lights have reversed each other [8–12]. Meanwhile, the spin direction of the photoelectron differs from the initial states when the excitation light has deviated from the p- and s-polarization conditions [10,12].

A lead atomic layer grown on a germanium (111) substrate [Pb/Ge(111)] is a prototypical example of a metallic surface state on a semiconductor substrate with a large Rashba spin splitting [13]. The surface structure of Pb/Ge(111) is well established, where one Pb atom is located at the H_3 site and three Pb atoms at the off-center bridge position between the T_1 and T_4 sites (Fig. 2a) [14–17]. The surface periodicity is $\left(\sqrt{3}\times\sqrt{3}\right)$R30°. The (11) plane is a mirror plane parallel to the $\bar{\Gamma}\bar{K}$ axis of the surface Brillouin zone of the $\left(\sqrt{3}\times\sqrt{3}\right)$R30° periodicity. The band structures along the $\bar{\Gamma}\bar{M}$ and $\bar{\Gamma}\bar{K}$ directions have been investigated by angle-resolved photoemission spectroscopy (ARPES), and several surface states have been reported [18]. Besides, the spin polarization of the metallic surface state in $\bar{\Gamma}\bar{M}$ is confirmed by both spin- and angle-resolved photoemission spectroscopy (SARPES) and theoretical calculations [13]. However, the spin polarization in the $\bar{\Gamma}\bar{K}$ direction has not been investigated. The $\bar{\Gamma}\bar{K}$ direction of the $\left(\sqrt{3}\times\sqrt{3}\right)$R30° periodicity is parallel to the mirror plane of the crystal. Thus, the spin-split electronic states in the $\bar{\Gamma}\bar{K}$ direction are suitable for the demonstration of the quantum interference in the photoexcitation process based on the mirror symmetry.

Received 22 January 2024; Revised 15 April 2024; Editorial Decision 19 April 2024; Accepted 22 April 2024

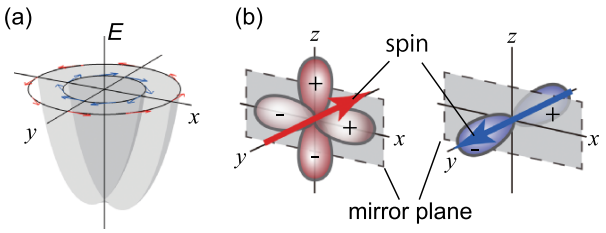

Fig. 1. (a) Schematic drawing of the Rashba-type spin-split bands. The arrows represent the spin texture of the bands. (b) Illustration of the spin-orbit coupling with the mirror symmetry. The symmetric orbitals are coupled to the $+y$-spin component, while the anti-symmetric orbitals are coupled to the $-y$-spin component. The linear combination of these states describes the total wavefunction of the system.

In the present study, we report on the spin polarization of photoelectrons emitted from the surface states o Pb/Ge(111) excited by a linearly polarized light investigated by SARPES. The spin polarization of the photoelectrons in the $\bar{\Gamma}\bar{K}$ mirror plane reverses between the p- and s-polarized lights. Furthermore, the spin direction of the photoelectron is modulated from that of the initial state when the electric field vector of the linearly polarized light deviates from the p- or s-polarization conditions. The changes in the spin polarization of photoelectrons are attributed to the quantum interference in the photoexcitation process. We demonstrate that the spin direction of photoelectrons can be controlled by orbital-selective photoexcitation from strongly spinorbit coupled surface states with polarized lights. The present concept is applicable to spin-polarized electron sources.

Methods

Experiments were conducted in an ultra-high vacuum environment with a base pressure of $<1\times10^{-8}$ Pa. The clean surface of the Ge(111) substrate was prepared by repeated cycles of Ar^+ sputtering at 0.7 keV and subsequently annealing up to 600°C. The clean surface was confirmed by observing the sharp c(2×8)low-energy electron diffraction pattern. Using a crucible-type evaporator, Pb was deposited on the Ge(111) substrate at room temperature. After the deposition, the surface was annealed at 280°C to prepare a wide and ordered terrace. The amount of Pb atoms and the quality of the monoatomic layer films were confirmed by observing the band structure of Pb/Ge(111) with ARPES [18].

The ARPES and SARPES measurements were performed at the National Institute for Materials Science, Japan, and the Institute for Solid State Physics (ISSP), the University of Tokyo. In the measurements at the National Institute for Materials Science, we used the imaging-type spin-resolved photoemission microscopy (iSPEM) machine combined with a 10.9 eV laser [19,20]. The SARPES measurements with a polarization-variable laser were performed in ISSP [21]. The experimental geometry for SARPES is shown in Fig. 2(b). Samples were prepared *in situ* for both experiments. The energy and wavenumber resolutions for SARPES were set to 8 meV and 0.01 $Å^{-1}$, respectively. The sample temperature was kept at 30 K during the measurements.

Results and discussion

Figure 2(c) shows the Fermi surface mapping of Pb/Ge(111). The ARPES measurement with the iSPEM and the 10.9 eV laser enables quick Fermi surface mapping in a whole Brillouin zone. The ARPES with a 6.994 eV laser provides a high-resolution image. We find a Pb-derived metallic surface state with a Rashba spin splitting (outer surface state: $S_{1,OSS}$, inner surface state: $S_{1,ISS}$). For the photoexcitation with $h\nu = 21.2$ eV, the photoelectron intensities from $S_{1,OSS}$ and $S_{1,ISS}$ in the second Brillouin zone are prominent [18]. In contrast, the photoexcitation with $h\nu = 6.994$ eV and $h\nu = 10.9$ eV yields sufficient photoelectron intensity even in the first surface Brillouin zone. The Fermi surfaces of $S_{1,OSS}$ and $S_{1,ISS}$ are strongly distorted due to the lattice potential. Here, the Fermi surface shape of $S_{1,ISS}$ is hexagonal while that of $S_{1,OSS}$ is dodecagonal and is warped inward.

Figure 2(d) exhibits the ARPES intensity mapping measured in the $\bar{\Gamma}\bar{K}$ direction. The S_2 and S_3 bands appear in addition to $S_{1,OSS}$ and $S_{1,ISS}$. The observed ARPES image agrees well with the calculated band structure shown in the literature 18. According to the calculation, S_2 and S_3 are also attributed to the Pb-derived states. On the other hand, the Ge-derived states appear around $\bar{\Gamma}$. Among these, the bands near the Fermi level are two-dimensional states with charge density distribution in the Ge subsurface region. According to previous studies [22–24], the Ge-derived subsurface states exhibit spin splitting due to the Rashba effect. The resolution of the SARPES used in the present study is significantly improved compared with that in the literature [24], and thus the spin polarization of the Ge subsurface states is clearly visualized.

In SARPES measurements, we analyze the spin of the photoelectrons emitted in the mirror plane (Fig. 2b). The light incident plane is parallel to the mirror plane of the sample, where the plane spanned by the light incident axis and the normal axis of the sample surface is defined as the incident plane. Figure 3(a, b) displays the SARPES image along the $\bar{\Gamma}\bar{K}$ mirror plane taken with the p- and s-polarized lights. The y-spin component, which is the spin polarization direction predicted by the Rashba effect and is perpendicular to the mirror plane, is detected in these images. We find the spin oriented in the $-y$ ($+y$) direction for $S_{1,ISS}$ and S_2 ($S_{1,OSS}$ and S_3) with the p-polarized light. In contrast, the observed spin polarization direction is reversed by switching the light polarization from p to s.

To understand the experimental result, we consider the dipole selection rule in photoexcitation. This treatment is analogous to those in Bi_2Se_3(111) and Bi(111) [10,12]. The photoelectron intensity is given by the formula of $I \propto |\langle\psi_f|\mathbf{A}\cdot\mathbf{p}|\psi_i\rangle|^2$, where $|\psi_i\rangle$ is the initial state, $|\psi_f\rangle$ the final state, $\mathbf{A}$ the vector potential of the incident light, and $\mathbf{p}$ the electron momentum operator. Here, we treat the photoexcitation in the mirror plane. The final state is assumed to be free-electron-like, which is symmetric with respect to the mirror plane. In order to guarantee a finite value for the matrix element, the initial state must be symmetric wavefunctions $|\psi_{sym}\rangle$ (anti-symmetric wavefunctions $|\psi_{asym}\rangle$ with respect to the mirror plane in the photoexcitation with the p-polarized (s-polarized) light. Therefore, the spin orientation reversal in the p- and s-polarized light excitations means that the $|\psi_{sym}\rangle$

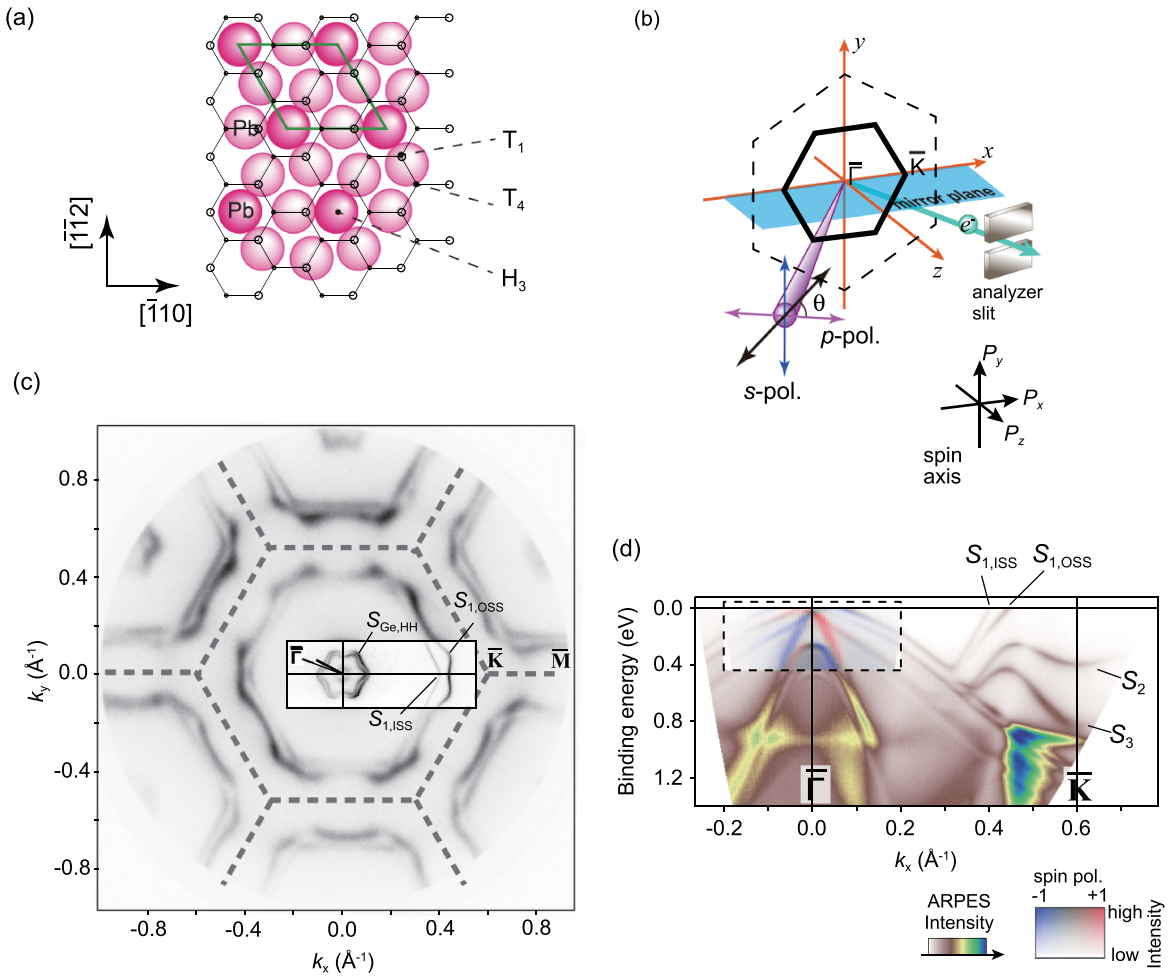

Fig. 2. (a) Atomic structure model of Pb/Ge(111). Large (small) balls represent the Pb (Ge) atoms. The parallelogram shows a $\left(\sqrt{3}\times\sqrt{3}\right)$R30° unit cell of Pb/Ge(111). (b) Schematic drawing of the experimental geometry. (c) The Fermi surface mapping of Pb/Ge(111) taken with the 10.9 eV laser. In the inset, a high-energy resolution image measured with a 6.994 eV laser is exhibited. The dotted lines denote the surface Brillouin zone boundary. (d) The angle-resolved photoemission spectroscopy intensity mapping recorded along the $\bar{\Gamma}\bar{K}$ mirror plane with the spin- and angle-resolved photoemission spectroscopy image around $\bar{\Gamma}$ near the Fermi level. The color table represents the photoelectron intensity and spin polarization information.

and $|\psi_{\mathrm{asym}}\rangle$ states are coupled to spins that are in mutually opposite directions (Fig. 3c, d).

The electronic states in solids are given by a linear combination of orbital eigen wavefunctions. In strongly spin-orbit coupled surface states, the spin direction depends on the symmetry of the orbital wavefunctions. Especially, as a general description of the mirror symmetry, the wavefunction of the surface state in the mirror plane is expressed as a linear combination of the symmetric and asymmetric wavefunctions with respect to the mirror plane, which are coupled to the spins in mutually opposite directions perpendicular to the mirror plane [10]. The spin-orbit coupled surface states of Pb/Ge(111) can also be explained by this scenario. In the present study, the spins of the surface states in the mirror plane must be oriented in the $\pm y$ direction since the mirror plane is defined as the x–z plane. Hereafter, the symmetric (anti-symmetric) orbitals coupled to the spin pointing to the $+y$ ($-y$) direction is described as $|\psi_{\mathrm{sym},\uparrow}\rangle$ ($|\psi_{\mathrm{asym},\downarrow}\rangle$). We note that the total spin polarization in the surface state is not to be one due to the spin–orbit coupling but depends on the weights of the symmetric and anti-symmetric orbital wavefunctions.

In the above discussion, we have treated the photoexcitation under the mirror symmetry, in which the mirror plane of the crystal, the light incident plane and the detection plane of the photoelectrons have been parallel to each other. The electric field vector of the incident light has also been symmetric, i.e. parallel for the p-polarized light or perpendicular for the s-polarized light, with respect to these planes. Next, we consider the rotation of the electric field vector of the linearly polarized light between p- and s-polarizations, as shown in the upper panel of Fig. 4. Here, the angle formed by the electric field vector with respect to the light incident plane is denoted as θ (Fig. 2b). In this case, the electric field vector of the light breaks the mirror symmetry, and photoelectron spins can be modified in the photoemission process.

Figure 4(a, b) shows the θ dependence of the spin polarization of the photoelectrons emitted from $S_{1,\mathrm{OSS}}$ at a wave number $\#k_1$ in the $\bar{\Gamma}\bar{K}$ mirror plane. The x, y and z components of the spin polarization are denoted P_{x}, P_{y} and P_{z}, respectively. The P_{y} value is 1 (−1) at $\theta = 0°$ and 180° ($\theta = 90°$), corresponding to the p-polarized (s-polarized) light. This spin polarization of the photoelectrons reflects the initial state information. The P_{y} value decreases when the electric field

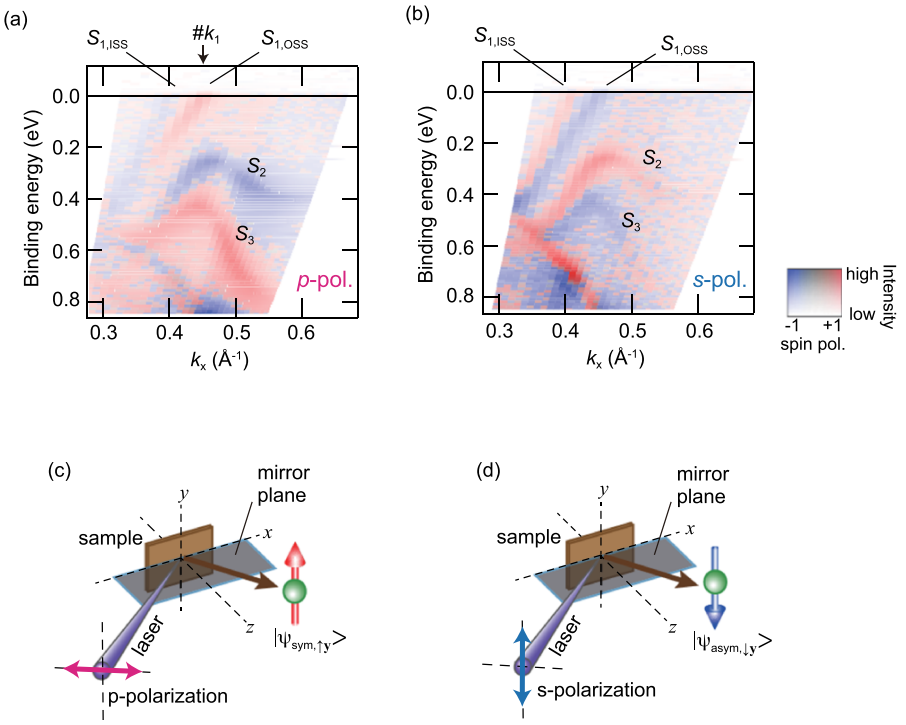

Fig. 3. (a and b) Spin- and angle-resolved photoemission spectroscopy images along $\bar{\Gamma}\bar{K}$ taken with the p- and s-polarized lights. The color table represents both the photoelectron intensity and the spin polarization. (c and d) Schematic drawing of the photoexcitation in the mirror plane with the p- and s-polarized lights. The light incident plane is parallel to the crystal mirror plane, and the photoelectrons emitted in the mirror plane are detected. The p-polarized (s-polarized) light excites the symmetric (anti-symmetric) orbitals coupled to the $+y$ ($-y$) spin component.

vector of the light is rotated from p to s polarization conditions and is to be 0 around $\theta = 60^\circ$ and 120°. The P_x and P_z values appear by rotating the electric field vector of the light, where P_x is prominent and P_z is small. These spin polarizations of the photoelectron do not reflect those of the initial state. The magnitude of the spin vector of the photoelectron can be obtained from the equation: $|\mathbf{P}| = \sqrt{P_x^2 + P_y^2 + P_z^2}$. We find that $|\mathbf{P}|$ is unity regardless of θ (Fig. 4c). This indicates that the spin vector of the photoelectrons rotates depending on θ.

We discuss the rotation of the spin vector of photoelectrons in the photoemission process and the appearance of a spin polarization component different from the initial state. The incident light has both p- and s-polarization components since the electric field vector of the light is tilted with respect to the light incident plane. Thus, the photoexcitation processes from $|\psi_{sym,\uparrow}\rangle$ and $|\psi_{asym,\downarrow}\rangle$ shown in Fig. 3(c, d) occur simultaneously. In a simple consideration, one might expect that the spin polarization of the photoelectrons in the y direction is reduced by the cancellation of spins pointing to the $+y$ and $-y$ directions. This mechanism can explain the experimentally observed decrease in P_y. In this scenario, one counts the number of spin-up and spin-down electrons, and the electron spins are treated incoherently. However, this mechanism does not explain the appearance of $P_{x,z}$. The optical transition we consider here is the simultaneous excitation of the spin-orbit coupled states $|\psi_{sym,\uparrow}\rangle$ and $|\psi_{asym,\downarrow}\rangle$ to the final states (Fig. 5a). In this process, there are two different excitation paths originating from the parity selection rule of the optical transition although the initial and final states have the same energy and wavenumber, respectively. Therefore, the photoexcitation must be treated as a coherent process. The $P_{x,z}$ components appear due to the superposition of simultaneously excited spins pointing to the $+y$ and $-y$ directions in the photoexcitation process. The spin polarization $P_{x,y,z}$ of the photoelectrons observed in Pb/Ge(111) is well reproduced by considering the quantum interference in the photoexcitation process shown in [10].

The superposition of spinors pointing to the $+y$ direction ($|\uparrow_y\rangle = \begin{pmatrix}1\\0\end{pmatrix}$) and the $-y$ direction ($|\downarrow_y\rangle = \begin{pmatrix}0\\-1\end{pmatrix}$) is described as $\cos\frac{\xi}{2}|\uparrow_y\rangle + \sin\frac{\xi}{2}e^{i\varphi}|\downarrow_y\rangle$, where φ is the phase difference of the weight coefficients of the linear combination, $\cos\frac{\xi}{2}$ and $\sin\frac{\xi}{2}$ are their absolute values. The meaning of this equation can be understood by using the Bloch sphere shown in Fig. 5(b). We take the spinors $|\uparrow_y\rangle$ and $|\downarrow_y\rangle$ at the north and south poles of the Bloch sphere, respectively. In this case, the spinors oriented in the x [z] direction are represented by $\frac{1}{\sqrt{2}}\begin{pmatrix}1\\\pm 1\end{pmatrix}\left[\frac{1}{\sqrt{2}}\begin{pmatrix}1\\\pm i\end{pmatrix}\right]$. The superposition of $|\uparrow_y\rangle$ and $|\downarrow_y\rangle$ is in the equatorial plane of the Bloch sphere if the absolute values of the weight coefficients are equal. Besides, the spinorin any direction can be produced by varying the absolute values of the weight coefficients. Therefore, in the present case, the weight coefficients of the simultaneously excited $|\psi_{sym,\uparrow}\rangle$ and $|\psi_{asym,\downarrow}\rangle$ can be varied by rotating the electric field vector of the linearly polarized light to change the ratio of the p- and s-polarized light components. This indicates that the spin direction of the photoelectron can be controlled by θ.

The spin vector rotation of the photoelectron excited from $S_{1,OSS}$ in Pb/Ge(111) with varying θ is depicted by the thick

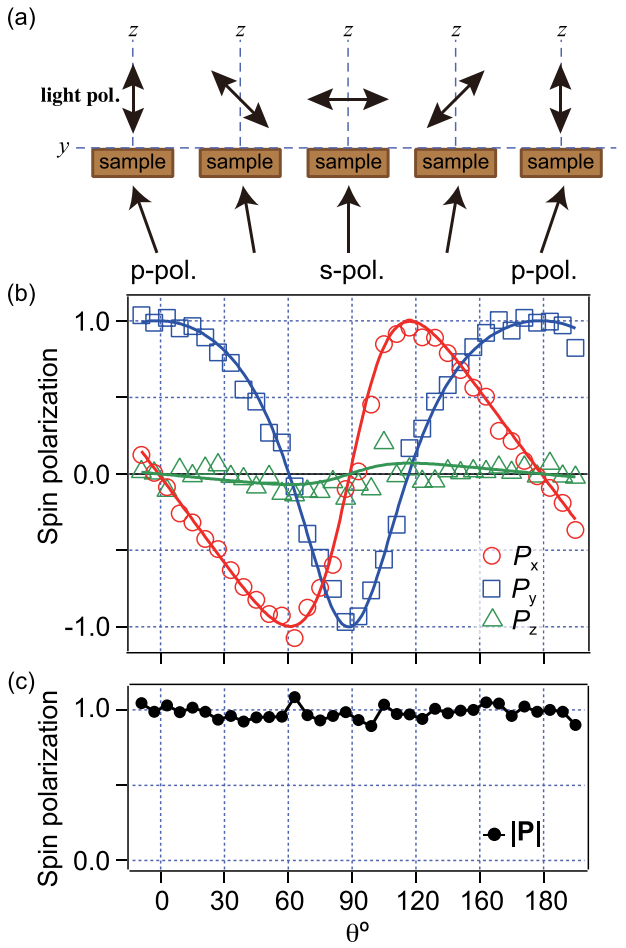

Fig. 4. (a) Illustration of the relationship between the electric field vector and the mirror plane. The θ dependence of the spin polarization of the photoelectrons (b) and the photoelectron intensity (c) emitted from $S_{1,OSS}$ at $\#k_1$ (Fig. 3a). The spin polarization is three-dimensionally analyzed. Circle, square and triangle symbols represent the *x*, *y* and *z* components of the spin polarization, respectively. Solid curves are the fitting results with the equations for the spin polarization of the photoelectron.

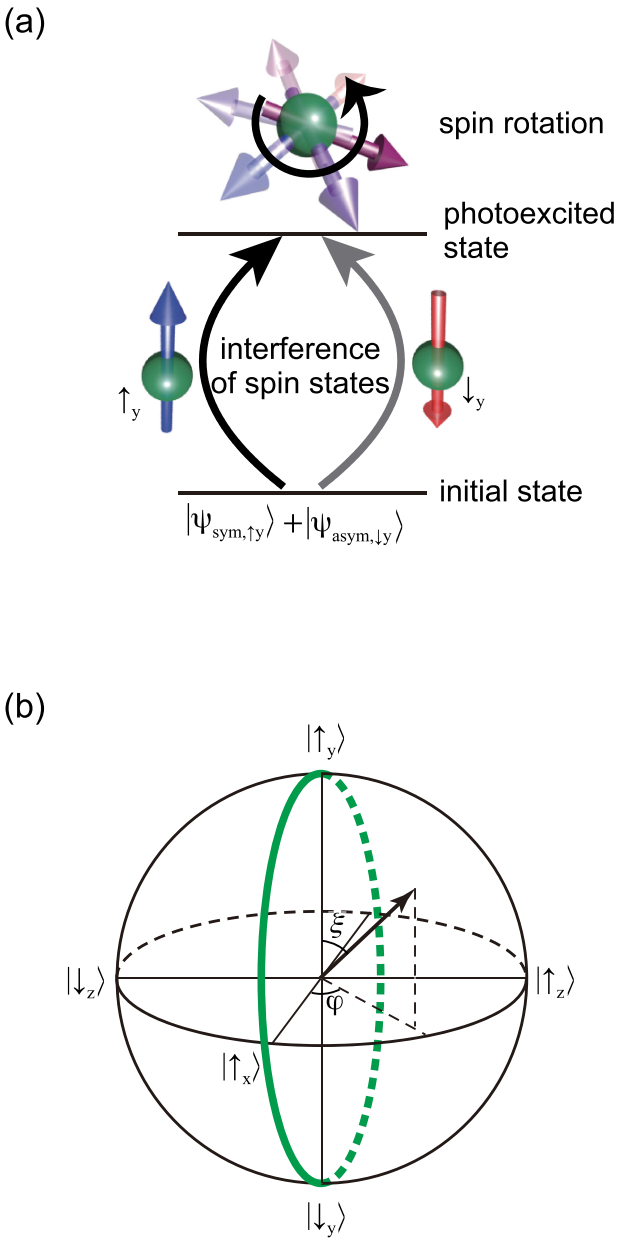

Fig. 5. (a) Illustration of the spin vector rotation due to the interference of the spin state between simultaneously photoexcited $|\psi_{sym,\uparrow}\rangle$ and $|\psi_{asym,\downarrow}\rangle$. (b) Diagram of the interference of spin states using a Bloch sphere. The spin quantization axis is defined in the *y* direction. The bold ellipse represents the variation of the spin vector direction of photoelectrons emitted from $S_{1,OSS}$ with changing θ.

ellipse in Fig. 5(b). The spin vector rotation in the photoexcitation process is also demonstrated in the spin-orbit coupled surface states of Bi(111) and Bi_2Se_3(111) [10,12]. We find the different spin vector rotations in the different systems. The quantum interference in the photoexcitation process depends on the details of the electronic state of the material. Various spin vector rotations of photoelectrons can be created by choosing materials with appropriate bands. Furthermore, photoexcitation with circularly or elliptically polarized lights offers a different spin vector rotation from that with linearly polarized light [25].

The concept revealed in the present study can be applicable to spin-polarized electron sources. The development of spin-polarized electron sources is underway to extract and control highly spin-polarized electrons. The concept of the optical spin control using the spin-orbit coupled surface states and the light polarization essentially allows the extraction of 100% spin-polarized photoelectrons with any spin direction. In the development of the cathode, one chooses a material whose electronic state is described as a mixture of the strongly spin-orbit coupled states $|\psi_{sym,\uparrow}\rangle$ and $|\psi_{asym,\downarrow}\rangle$. The combination of the cathode material and the polarization control of the light produces various spin-polarized photoelectrons.

In the present study, we treat the photoelectron spin emitted into the vacuum. By lowering the excitation energy, the electrons can be excited into the conduction band, retaining them in the materials. We consider that the basic physics for the optical spin control is common even for the photoexcited electrons in the conduction band. If one can control the spin of electrons in the conduction band, the potential applications significantly expand. The optical spin control based on the quantum interference would open new pathways for future spintronics.

Concluding remarks

We have reported the results of the ARPES and SARPES measurements of Pb/Ge(111). For the photoexcitation with the p- and s-polarized lights, the spin polarization is observed in the direction perpendicular to the mirror plane, and the direction is reversed. The surface states in the mirror plane of Pb/Ge(111) are described by a linear combination of $|\psi_{sym,\uparrow}\rangle$ and $|\psi_{asym,\downarrow}\rangle$, similar to other strongly spin-orbit coupled systems such as Bi(111) and Bi_2Se_3(111). The photoelectron spin is oriented in a different direction from the initial-state spin, depending on the direction of the electric field of the incident light. This is due to the quantum interference between simultaneously excited $|\psi_{sym,\uparrow}\rangle$ and $|\psi_{asym,\downarrow}\rangle$ in the photoexcitation process. Tremendous efforts are made to control the spin direction by using the spin-orbit interaction, most of which focus solely on the spin structure in the initial state. We propose a concept of spin control using interference of spin states in the photoexcitation process, where the matrix element of photoemission plays an important role in determining the spin vector direction of photoelectrons.

Acknowledgements

The authors thank Ayumi Harasawa and Fumiya Arai for their technical support in experiments at ISSP. The authors also thank Ryo Noguchi for sharing an Igor macro. SARPES experiments were performed in joint research with ISSP, the University of Tokyo.

Funding

Japan Society for the Promotion of Science KAKENHI (JP21K04633, JP21H04652, JP22H01761); Innovative Science and Technology Initiative for Security Grant Number (JPJ004596); ATLA, Japan; Iketani Science and Technology Foundation.

Conflicts of interest

The authors declare that they have no conflict of interest.

Data availability

The data underlying this article are available from the corresponding author upon reasonable request.

References

1. Nowack K C, Koppens F H, Nazarov Y V, and Vandersypen L M (2007) Coherent control of a single electron spin with electric fields. *Science* 318: 1430–1433.
2. Hanson R and Awschalom D D (2008) Coherent manipulation of single spins in semiconductors. *Nature* 453: 1043–1049.
3. Awschalom D D, Bassett L C, Dzurak A S, Hu E L, and Petta J R (2013) Quantum spintronics: engineering and manipulating atom-like spins in semiconductors. *Science* 339: 1174–1179.
4. Yazyev O V, Moore J E, and Louie S G (2010) Spin polarization and transport of surface states in the topological insulators Bi_2Se_3 and Bi_2Te_3 from first principles. *Phys. Rev. Lett.* 105: 266806.
5. Zhu Z H, Veenstra C N, Levy G, Ubaldini A, Syers P, Butch N P, Paglione J, Haverkort M W, Elfimov I S, and Damascelli A (2013) Layer-by-layer entangled spin-orbital texture of the topological surface state in Bi_2Se_3. *Phys. Rev. Lett.* 110: 216401.
6. Cao Y, Waugh J A, Zhang X W, Luo J W, Wang Q, Reber T J, Mo S K, Xu Z, Yang A, Schneeloch J, Gu G D, Brahlek M, Bansal N, Oh S, Zunger A, and Dessau D S (2013) Mapping the orbital wavefunction of the surface states in three-dimensional topological insulators. *Nat. Phys.* 9: 499–504.
7. Zhang H, Liu C X, and Zhang S C (2013) Spin-orbital texture in topological insulators. *Phys. Rev. Lett.* 111: 066801.
8. Xie Z, He S, Chen C, Feng Y, Yi H, Liang A, Zhao L, Mou D, He J, Peng Y, Liu X, Liu Y, Liu G, Dong X, Yu L, Zhang J, Zhang S, Wang Z, Zhang F, Yang F, Peng Q, Wang X, Chen C, Xu Z, and Zhou X J (2014) Orbital-selective spin texture and its manipulation in a topological insulator. *Nat. Commun.* 5: 3382.
9. Zhu Z H, Veenstra C N, Zhdanovich S, Schneider M P, Okuda T, Miyamoto K, Zhu S Y, Namatame H, Taniguchi M, Haverkort M W, Elfimov I S, and Damascelli A (2014) Photoelectron spin-polarization control in the topological insulator Bi_2Se_3. *Phys. Rev. Lett.* 112: 076802.
10. Yaji K, Kuroda K, Toyohisa S, Harasawa A, Ishida Y, Watanabe S, Chen C T, Kobayashi K, Komori F, and Shin S (2017) Spin-dependent quantum interference in photoemission process from spin-orbit coupled states. *Nat. Commun.* 8: 14588.
11. Jozwiak C, Park C H, Gotlieb K, Hwang C, Lee D H, Louie S G, Denlinger J D, Rotundu C R, Birgeneau R J, Hussain Z, and Lanzara A (2013) Photoelectron spin-flipping and texture manipulation in a topological insulator. *Nat. Phys.* 9: 293–298.
12. Kuroda K, Yaji K, Nakayama M, Harasawa A, Ishida Y, Watanabe S, Chen C T, Kondo T, Komori F, and Shin S (2016) Coherent control over three-dimensional spin polarization for the spin-orbit coupled surface state of Bi_2Se_3. *Phys. Rev. B* 94: 165162.
13. Yaji K, Ohtsubo Y, Hatta S, Okuyama H, Miyamoto K, Okuda T, Kimura A, Namatame H, Taniguchi M, and Aruga T (2010) Large Rashba spin splitting of a metallic surface-state band on a semiconductor surface. *Nat. Commun.* 1: 17.
14. Huang H, Wei C M, Li H, Tonner B P, and Tong S Y (1989) Quantitative structural determination of metallic film growth on a semiconductor crystal: $(\sqrt{3} \times \sqrt{3})R30^\circ \rightarrow (1\times1)$ Pb on Ge(111). *Phys. Rev. Lett.* 62: 559–562.
15. Ancilotto F, Selloni A, and Car R (1993) β-phase of Pb on Ge(111): the competing roles of electronic bonding and thermal fluctuations. *Phys. Rev. Lett.* 71: 3685–3688.
16. Vries S A, Goedtkindt P, Steadman P, and Vlieg E (1999) Phase transition of a Pb monolayer on Ge(111). *Phys. Rev. B* 59: 13301.
17. Ohtsubo Y, Muto H, Yaji K, Hatta S, Okuyama H, and Aruga T (2011) Structure determination of Pb/Ge(111)-β-by dynamical low-energy electron diffraction analysis and first-principles calculation. *J. Phys. Condens. Matter* 23: 435001.
18. Yaji K, Hatta S, Aruga T, and Okuyama H (2012) Structural and electronic properties of the Pb/Ge(111)-β surface studied by photoelectron spectroscopy and first-principles calculations. *Phys. Rev. B* 86: 235317–245422.
19. Yaji K and Tsuda S (2024) Development of a photoemission microscopy apparatus using a vacuum ultraviolet laser. e-J. *Surf. Sci. Nanotechnol.* 22: 46–52.
20. Yaji K and Tsuda S (2024) Visualization of spin-polarized electronic states by imaging-type spin-resolved photoemission microscopy. *Sci. Technol. Adv. Mater.* 4: 2328206.
21. Yaji K, Harasawa A, Kuroda K, Toyohisa S, Nakayama M, Ishida Y, Fukushima A, Watanabe S, Chen C T, Komori F, and Shin S (2016) High-resolution three-dimensional spin- and angle-resolved photoelectron spectrometer using vacuum ultraviolet laser light. *Rev. Sci. Instrum.* 87: 053111.
22. Ohtsubo Y, Hatta S, Yaji K, Okuyama H, Miyamoto K, Okuda T, Kimura A, Namatame H, Taniguchi M, and Aruga T (2010)

Spin-polarized semiconductor surface states localized in subsurface layers. *Phys. Rev. B* 82: 201307(R).
23. Ohtsubo Y, Yaji K, Hatta S, Okuyama H, and Aruga T (2013) Two-dimensional states localized in subsurface layers of Ge(111). *Phys. Rev. B* 88: 245310.
24. Yaji K, Ohtsubo Y, Hatta S, Okuyama H, Yukawa R, Matsuda I, Fèvre Le P, Bertran F, Taleb-Ibrahimi A, Kakizaki A, and Aruga T (2015) Experimental evidence for two-dimensional states localized in subsurface region of Ge(111). *J. Elec. Spec. Rel. Phenom.* 201: 92–97.
25. Kuroda K, Yaji K, Noguchi R, Harasawa A, Shin S, Kondo T, and Komori F (2022) Visualization of optical polarization transfer to photoelectron spin vector emitted from a spin-orbit coupled surface state. *Phys. Rev. B* 105: L121106.